

# Geostatistical Analysis for Magnitude Scale Conversion and Gutenberg-Richter Parameter Estimation: Insights from Regional Seismicity of Nubian-Eurasian Plate Boundary Region

Peter Adetokunbo<sup>1</sup>, Ayodeji Adekunle Eluyemi<sup>2\*</sup>, Eniolayimika Jegede<sup>3</sup>, Segun Aguda<sup>4</sup>, Tunji Omoseyin<sup>5</sup>, Debasis D. Mohanty<sup>6</sup>, Manzunzu Brassnavy<sup>7</sup>, Paulina Amponsah<sup>8</sup>, Saurabh Baruah<sup>6</sup>

<sup>1</sup>Boone Pickens School of Geology, Oklahoma State University, Stillwater, OK 74078, USA

<sup>2</sup>Division of Environment and Earth Science, Centre for Energy Research and Development (CERD), Obafemi Awolowo University (OAU), Ile-Ife, Nigeria

<sup>3</sup>Areleos Global Enterprise, Huntsville, Texas, USA

<sup>4</sup>Department of Project Management, Missouri State University, Springfield, Missouri State, USA

<sup>5</sup>Department of Safety Sciences and Environmental Engineering, Indiana University of Pennsylvania, Indiana Pennsylvania, USA

<sup>6</sup>Geosciences and Technology Division, CSIR—North East Institute of Science and Technology (CSIR-NEIST), Jorhat-785006, Assam, India

<sup>7</sup>National University of Science and Technology, Bulawayo, Zimbabwe

<sup>8</sup>School of Nuclear and Allied Sciences, Ghana Atomic Energy Commission, Accra, Ghana

Email: \*ay\_dot2006@yahoo.com

**How to cite this paper:** Adetokunbo, P., Eluyemi, A. A., Jegede, E., Aguda, S., Omoseyin, T., Mohanty, D. D., Brassnavy, M., Amponsah, P., & Baruah, S. (2025). Geostatistical Analysis for Magnitude Scale Conversion and Gutenberg-Richter Parameter Estimation: Insights from Regional Seismicity of Nubian-Eurasian Plate Boundary Region. *Journal of Geoscience and Environment Protection*, 13, 230-248.

<https://doi.org/10.4236/gep.2025.137014>

**Received:** April 28, 2025

**Accepted:** July 21, 2025

**Published:** July 24, 2025

## Abstract

This work presents the analyses of earthquake magnitude scales and seismicity parameters across the Nubian-Eurasian Plate Boundary Region. We developed magnitude conversion models using three regression techniques ( $R^2 \approx 0.68$ ) and implemented a tapered Gutenberg-Richter model with bootstrap uncertainty quantification. Our analysis yielded  $M_c = 4.35$ ,  $b$ -value = 0.93 (95% CI: 0.74 - 1.09),  $a$ -value = 6.19 (95% CI: 5.35 - 6.90), corner magnitude = 8.69 (95% CI: 5.77 - 8.69), and maximum magnitude ( $M_{max}$ ) = 7.24 (95% CI: 6.50 - 7.24). The tapered model provides superior fitting at higher magnitudes compared to the standard Gutenberg-Richter relationship, addressing a key limitation in seismic hazard characterization. The  $b$ -value below 1.0 indicates elevated potential for higher-magnitude events, while the substantial  $a$ -value suggests significant seismic productivity across the boundary. The relatively high  $M_c$  value points to limitations in detecting smaller earthquakes, particularly in less-instrumented areas of the boundary zone. The estimated  $M_{max}$  and corner magnitude constrain the upper bound of potential earthquake magnitudes, critical

Copyright © 2025 by author(s) and Scientific Research Publishing Inc. This work is licensed under the Creative Commons Attribution International License (CC BY 4.0). <http://creativecommons.org/licenses/by/4.0/>



Open Access

for hazard assessments and engineering applications. While treating the region as a single seismotectonic unit was necessary given current data constraints, we acknowledge this approach's limitations given the boundary's diverse tectonic regimes. Future research should develop zone-specific parameters that account for distinct regional characteristics. Nevertheless, these region-wide parameters establish a valuable baseline framework for seismic hazard assessment, particularly useful where zone-specific data remain insufficient.

## Keywords

Magnitude Conversion, Gutenberg-Richter Parameters, Machine Learning, Seismic Hazard, b-Value, Magnitude of Completeness, Nubian-Eurasian Plate Boundary

## 1. Introduction

Earthquake magnitude estimation forms an integral part of seismic event analysis and is an essential input for seismic hazard assessments and regional tectonic analyses (Agharroud et al., 2021; Montilla et al., 2003; Cherkaoui & El Hassani, 2012). Determination of earthquake magnitude is especially critical at the convergent Nubian-Eurasian tectonic plate region, which features elevated seismic activity and complex tectonics stretching from the Atlantic coastal region of Morocco, passing through southern Iberia, and including the western Mediterranean. The September 8, 2023, earthquake of magnitude 6.8 and its implications for the Marrakesh region's High Atlas Mountains highlight an urgent need for extensive seismic appraisal for the area.

In the historical record of seismic monitoring across Nubian-Eurasia, a multitude of magnitude scales have hitherto been utilized, including surface wave magnitude ( $M_s$ ), body wave magnitude ( $m_b$ ), local magnitude ( $M_L$ ), and moment magnitude ( $M_w$ ) (El Alami et al., 1998). Use of myriad methodologies for magnitude estimation poses great challenges to consistent compilation of earthquake catalogs, a necessary activity for proper seismic hazard appraisal. Previous studies have attempted to address this problem through a variety of measures. Peláez et al. (2007) and Hamdache et al. (2010) compiled large catalogs with major earthquakes in Morocco and Northern Algeria, respectively, which include seismic events dating back to the 11th century. While these historical catalogs focused upon modern seismic hazard and shed light upon inadequacies of available records, major challenges to achieving consistency amongst magnitude scales still hinder regional hazard assessments.

A major limitation of the available research is related to insufficient characterization of magnitude-frequency distributions, especially for larger magnitudes, which represent the most serious degree of hazard. Classic Gutenberg-Richter relations often fail to describe occurrences of larger seismic events for complex tectonic settings, including those at Nubian-Eurasia. Such shortcomings pose serious

issues as those larger, rarer events have a major impact on seismic hazard computation and development of engineering design criteria. Additionally, recent developments, as typified by Poggi's et al. (2020) North African seismic hazard model, acknowledge persisting issues related to estimation of parameters through heterogeneity of catalogues and lack of records of magnitude-frequency distributions at higher magnitudes.

Modeling is challenged by the complex tectonic dynamics at the junction of the Nubian and Eurasia plates. The boundary displays a changing trend from transform motion along the Atlantic to convergent tectonics along the Mediterranean, with microplate interactions giving rise to an assorted variety of fault systems, with different seismogenic characteristics. While researchers like Zitellini et al. (2009) and Chertova et al. (2014) have made maps of major fault structures and modeled tectonic evolution, translating geological observations to trustworthy seismic parameters requires use of more advanced statistical methods than are normally used.

The Gutenberg-Richter (GR) relation, which describes the frequency-magnitude distribution of seismic events, is pivotal to understanding seismicity patterns within the region. Determination of the exact values for those parameters characteristic of the Gutenberg-Richter relation, i.e., magnitude of completeness ( $M_c$ ), a-value (seismicity rate), and b-value (the ratio between larger and smaller earthquakes), is of utmost importance for performing effective seismic hazard evaluations (Pacheco et al., 1992; Frohlich & Davis, 1993; Wiemer & Schorlemmer, 2007). In addition, estimation of maximum likelihood earthquake magnitude ( $M_{max}$ ) puts critical constraints on both long-term hazard assessments and engineering design methods. All these parameters, together, provide invaluable information concerning stress regime and tectonic features of different segments of the Nubian-Eurasia plate boundary (Bada et al., 1998; Mousavi, 2017; Taroni & Carafa, 2023).

Current research addresses an important gap left by previous work in understanding magnitude and frequency connections through an application of tapered Gutenberg-Richter model with bootstrap uncertainty estimation. Such an approach successfully obviates constraints inherent with modeling large-magnitude earthquakes by creating a physically reasonable upper bound of earthquake size, as opposed to the infinite potential of power-law distribution of the original model. Not only do we represent decreasing occurrences of high-magnitude events realistically, but with good uncertainty estimations, we produce more realistic limits to seismic hazard parameters, which are essential for successful hazard mitigation within this heavily populated tectonic plate boundary region.

While the initial characterization of the region as an integrated seismotectonic structure is conceptually important, results of this study will significantly contribute to improved evaluations of key seismic characteristics and promote development of more sophisticated hazard assessment models for the various tectonic regimes around the Nubian-Eurasia plate boundary zone. Impacts of these results

are far-reaching for building codes, infrastructure development, and emergency preparedness for many urban areas bordering this active plate boundary.

## 2. Tectonic Setting of the Nubian-Eurasian

The Nubian-Eurasian tectonic plate boundary is a multidimensional geological setting that runs from the Atlantic, through Morocco, southern Iberia, and the Alboran Sea, and further eastward along the Mediterranean (**Figure 1**). It provides the context for the convergence of the Nubian and Eurasian tectonic plates, which manifests in a variety of structural features in its varied sections.

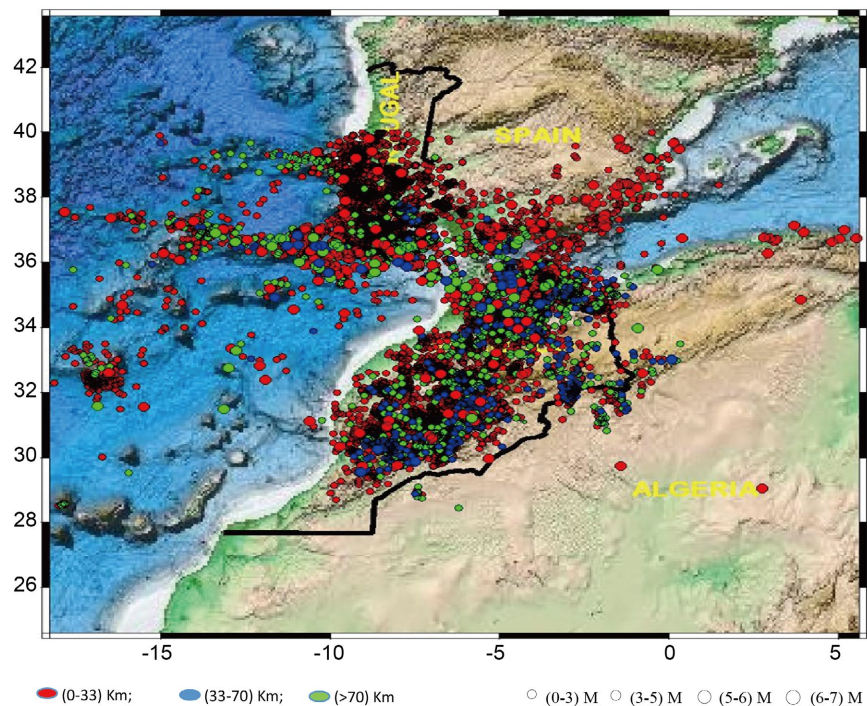


**Figure 1.** Epicentral plot of the Morocco earthquake events from 1979 to 2025.

The Moroccan High Atlas (MHA) forms a major intracontinental mountain range with substantial thick-skinned thrusting and folding, with geometry that reflects double divergence (Lanari et al., 2020). This has acted as an important accommodation zone for much of the Africa-Eurasia convergence since the Miocene era, placing it in a vast western Mediterranean plate boundary province (Gomez et al., 2000). The MHA has a gradient of tectonic shortening degree that decreases from the eastern part towards the western part (Teixell et al., 2003, 2017). Of particular interest, the western part of the MHA is heavily influenced by transgression regimes, as revealed in the South Atlas and North Atlas fault zones.

Toward the west, the Gulf of Cadiz serves as the transition region between the predominantly compressional tectonic activity found in the Mediterranean and the Atlantic transform-dominated segment. It is characterized by complex strain partitioning that comprises active thrust faulting systems, strike-slip mechanisms,

and associated deep-seated structural elements with the ability to generate strong seismic events, such as the destructive Lisbon earthquake of 1755 (Zitellini et al., 2009). The SWIM fault zone (Southwest Iberian Margin) comprises a chain of dextral strike-slip faults that accommodate the westward extrusion of crustal material (Terrinha et al., 2019).

Gibraltar Arc System includes the Betic Cordillera in southern Spain and the Rif Mountains in northern Morocco and marks a tight orogenic arc around the Alboran Sea. This part of the Earth experienced substantial crustal extension during the Miocene epoch but, at the same time, experienced compressional stress on its periphery—a paradox explained by a number of theoretical models such as lithospheric delamination, slab rollback, and removal of lithospheric material by convection (Platt et al., 2013; Chertova et al., 2014).

The clear instrumental and historic seismicity in the region exists as an indicator of the dynamic tectonic mechanisms associated with the neighboring plate boundary. Extensive earthquake databases compiled by Peláez et al. (2007) for Morocco and by Hamdache et al. (2010) for Northern Algeria show a substantial history of seismic activity with dates of 1045 CE and 856 CE, respectively, thus indicating the ongoing seismic hazard on different portions of the boundary. Recent seismic hazard assessments by Poggi et al. (2020) merge geodetic, geological, and seismological data into a multi-level model for North Africa that accommodates spatial variability of deformation rates, as well as the seismogenic character present in the extensively circumscribed region.

During the course of the Variscan orogen, widespread deformation occurred throughout the region, highlighted by the Tizi n'Test right-lateral strike-slip fault of Morocco region (Mattaueer et al., 1972), together with accompanying geological formations of southwestern Iberia. At the same time, the Anti-Atlas belt became a fold-and-thrust belt, leading to the re-activation of geological structures formed during the late Proterozoic-Precambrian time scales (Helg et al., 2004). The onset of extensional tectonics of the Permian time affected northwestern Africa and southern Iberia concurrently with the breakup of the African continent. The tectonic event led to rift development within the basins, especially during the Triassic and Jurassic periods (Arboleya et al., 2004; Lanari et al., 2020).

The northwest-southeast trending extension produced normal faults with a north-south direction, in addition to the reactivation of previously existing Variscan structures with northeast-southwest and east-northeast-west-southwest directions in the region. One prime example of such a reactivation is the Tizi n'Test fault, which became a left-lateral strike-slip fault over that period of time. Similar structural activations occurred in the southern Iberia region through the Trans-Alboran Shear Zone and accompanying faulting.

The Late Cretaceous was characterized by tectonic inversion across the boundary zone, from the Atlas mountain chains to the Betic-Rif orogen, due to compressional forces caused by the Africa-Eurasia convergence. The tectonic inversion episode significantly influenced the present-day structural layout of the re-

gion, thus contributing decisively to its complex geological evolution (Frizon de Lamotte et al., 2000). Present-day GPS measurements indicate that convergence continues at rates of 4 to 5 mm per year, and the motion is partitioned into compressional and strike-slip components along different segments of this active geological boundary (Koulali et al., 2011).

### 3. Data and Methodology

#### 3.1. Data Collection and Processing

This study examines a seismological dataset encompassing 9152 earthquake events documented in the Nubian-Eurasian plate boundary region from 1979 to 2025, acquired from the International Seismological Center (ISC). The data is plotted to reveal the epicentral distributions of the earthquake events in the region (Figure 1), around Morocco, Spain, and Portugal. The dataset underwent thorough processing to enhance the quality and consistency needed for parameter extraction. Data cleaning involved systematically removing records with missing values, particularly focusing on eliminating entries where body-wave magnitude (mb), local magnitude (ML) and moment magnitude (Mw) were not recorded, as these parameters are essential for magnitude conversion relationships. Notably, a significant portion of the original records lacked all the necessary parameters for our analysis framework. We implemented a cleaning process with Python routine. This program reads an Excel file containing seismic data and iterates through each row to find and read three types of earthquake magnitude data: Local Magnitude (ML), Body Wave Magnitude (mb), and Moment Magnitude (Mw), along with any other depth information. The operation here is to search each column in separate rows for magnitude type indicators (“ml”, “mb”, “mw”, “local magnitude”, “body wave”, etc.) and then extract the corresponding numerical values from adjacent columns. An important filtering condition is that only rows containing all three types of magnitudes (ML, mb and Mw) are retained, thus ensuring data completeness for further comparative analysis. After applying these quality control procedures, the dataset was condensed to 327 well-characterized events with complete magnitude information. This refined collection of seismic data, while smaller than the original catalog, provides high-quality records with multiple magnitude scales reported for the same events, serving as a cornerstone for investigating seismicity patterns and hazard evaluation in the region.

The methodology consists of two main components: (1) establishing empirical relationships between different magnitude scales, and (2) determining the Gutenberg-Richter parameters using multiple methods.

#### 3.2. Magnitude Scale Relationships

The significance of interrelationships among diverse magnitude scales cannot be overstated in the context of earthquake catalog unification. This study endeavors to formulate an empirical relationship between the moment magnitude (Mw) and two critical source parameters: body wave magnitude (mb), and local magnitude

(ML). **Table 1** shows the correlation matrix, indicating that both ML and mb are potentially significant predictors of Mw because of their strong individual correlations with the target variable. However, the moderate correlation between the predictors necessitates the examination of multicollinearity to ensure the reliability of the regression model. Appropriate diagnostic measures should be implemented to verify that multicollinearity does not negatively impact the model's performance. To address this issue, we implemented a triad of complementary regression techniques: Multiple Linear Regression (MLR), Huber Regression, and Elastic Net Regression. Subsequently, we applied a weighted averaging approach to synthesize the results.

**Table 1.** Correlation matrix of seismic magnitude scales.

Measurement	ML	mb	Mw
ML	1.0000	0.4665	0.7488
mb	0.4665	1.0000	0.6920
Mw	0.7488	0.6920	1.0000

### 3.2.1. Multiple Linear Regression

MLR is a statistical approach for establishing relationships between multiple variables, and in this case, between source parameters and moment magnitude (Castellaro et al., 2006). The model can be expressed as

$$Mw = \beta_0 + \beta_1 mb + \beta_2 ML + \varepsilon$$

where  $\beta_0$ ,  $\beta_1$ , and  $\beta_2$  are regression coefficients, and  $\varepsilon$  represents the error term. This model assumes a linear relationship between the predictor variables and Mw.

### 3.2.2. Huber Regression

Huber regression is utilized to address potential outliers in the magnitude data (Huber, 1992). This robust regression methodology combines the optimal properties of both the absolute error (L1) and squared error (L2) loss functions, rendering it less susceptible to outliers that are prevalent in seismic data. The Huber loss function for a single data point is defined as

$$L(r) = \begin{cases} \frac{1}{2}r^2, & \text{if } |r| \leq \delta \\ \delta \cdot (|r| - \delta/2), & \text{if } |r| > \delta \end{cases}$$

where  $r$  is the residual, and  $\delta$  is the hyperparameter that determines the transition point between the L1 and L2 losses.

### 3.2.3. Elastic Net Regression

Elastic net regression integrates L1 and L2 regularization techniques to mitigate potential multicollinearity among diverse magnitude scales, while preserving model stability. The objective function is expressed as (Zou & Hastie, 2005):

$$L(\beta) = \min \left( Y - X\beta^2 + \alpha \left[ (1-\lambda)\beta^2 + \lambda\beta_1 \right] \right)$$

where  $\alpha$  controls the overall regularization strength and  $\lambda$  balances the L1 and L2 penalties. This approach is especially valuable when handling potentially interrelated predictors such as mb and ML.

### 3.2.4. Magnitude Moment Estimation

The final moment magnitude estimate ( $M_w\_final$ ) was computed as the weighted average of the predictions from the three methods.

$$M_w\_final = w_1 M_w\_MLR + w_2 M_w\_Huber + w_3 M_w\_net$$

The weights  $w_1$ ,  $w_2$ , and  $w_3$  are determined based on the relative performance of each methodology, as assessed through cross-validation procedures and prediction error metrics. These weights were optimized to minimize prediction errors while ensuring model stability across diverse magnitude ranges.

The integration of multiple regression techniques in this ensemble approach enhances the robustness of the magnitude scale conversions for seismic hazard evaluation. By leveraging the strengths of the individual methods while counteracting their respective weaknesses, this strategy yields more reliable results.

### 3.3. Gutenberg-Richter Parameters

The second component involves determining the Gutenberg-Richter parameters. This fundamental relationship is expressed as follows:

$$\log_{10} N = a - bM$$

where  $N$  is the cumulative number of earthquakes with magnitude  $\geq M$ ,  $a$  represents the overall seismicity rate, and  $b$  describes the relative size distribution of the earthquakes (Gutenberg and Richter, 1944; Eluyemi et al., 2019).

The magnitude of completeness ( $M_c$ ) was determined using the maximum curvature technique, which identifies the magnitude bin with the highest frequency in the non-cumulative magnitude distribution. This approach provides an initial estimate that generally represents the lower bound of the true  $M_c$  (Wiemer & Wyss, 2000). We complemented this with a goodness-of-fit assessment that evaluates the coefficient of determination ( $R^2$ ) across a range of potential  $M_c$  values, selecting the threshold that maximizes this metric.

Following the identification of  $M_c$ , we implemented both the standard and tapered Gutenberg-Richter models. The standard b-value was calculated using the maximum likelihood method (Aki, 1965):

$$b = \frac{\log_{10}(e)}{\bar{m} - \left( M_c - \frac{\Delta M}{2} \right)}$$

where  $\Delta M$  is the magnitude bin width (typically 0.1) and  $\bar{m}$  is the mean magnitude of events above  $M_c$ .

The standard Gutenberg-Richter model, however, assumes an infinite power-law distribution of magnitudes, which is physically unrealistic. To address this

limitation, particularly for higher magnitudes that are critical for seismic hazard assessment, we implemented a tapered Gutenberg-Richter model. This model incorporates a tapering function that causes the distribution to decay more rapidly as magnitudes approach some physical maximum:

$$\log_{10} N(M) = a - bM + \log_{10} \left( e^{-\left(\frac{M-M_c}{\delta}\right)} \right)$$

where the additional exponential term represents the tapering effect, with parameters for corner magnitude and maximum magnitude ( $M_{\max}$ ).

We also implemented bootstrap statistics to quantify uncertainty in all Gutenberg-Richter parameters, not just  $M_{\max}$ . The bootstrap method is recognized as a robust non-parametric approach for uncertainty quantification of seismic hazard parameters (Efron & Tibshirani, 1993; Orlecka-Sikora, 2008). Following methodologies developed by Lasocki and Orlecka-Sikora (2008), we generated 1,000 artificial catalogs by means of random sampling with replacement from the initial earthquake catalog, specifically those events above the completeness threshold.

For each bootstrap sample, we calculated estimates of all key parameters: a-value (productivity), b-value (relative size distribution), corner magnitude (where tapering begins), and maximum magnitude ( $M_{\max}$ ). The bootstrap procedure yielded distributions for each parameter, enabling us to derive: (1) mean values representing central tendency, (2) 95% confidence intervals quantifying uncertainty bounds, and (3) comprehensive assessment of potential parameter variability across the tapered Gutenberg-Richter model.

This approach is particularly valuable for characterizing b-value stability across the study region and for determining a statistically robust estimate of maximum magnitude. The bootstrap method's strength lies in avoiding assumptions about underlying parametric distributions, making it exceptionally suitable for the typically limited earthquake catalog datasets (Kijko & Singh, 2011). The technique is especially important because the standard Gutenberg-Richter relationship often fails to adequately model the distribution of larger magnitude events, which are critical for hazard assessment.

The tapered model parameters derived through bootstrap analysis provide insight into the physical constraints on earthquake size in the Nubian-Eurasian plate boundary region. The corner magnitude parameter indicates where the distribution begins to deviate from the standard power-law relationship, while the maximum magnitude parameter establishes an upper bound that reflects the region's seismogenic potential. Both parameters benefit from the uncertainty quantification provided by the bootstrap approach.

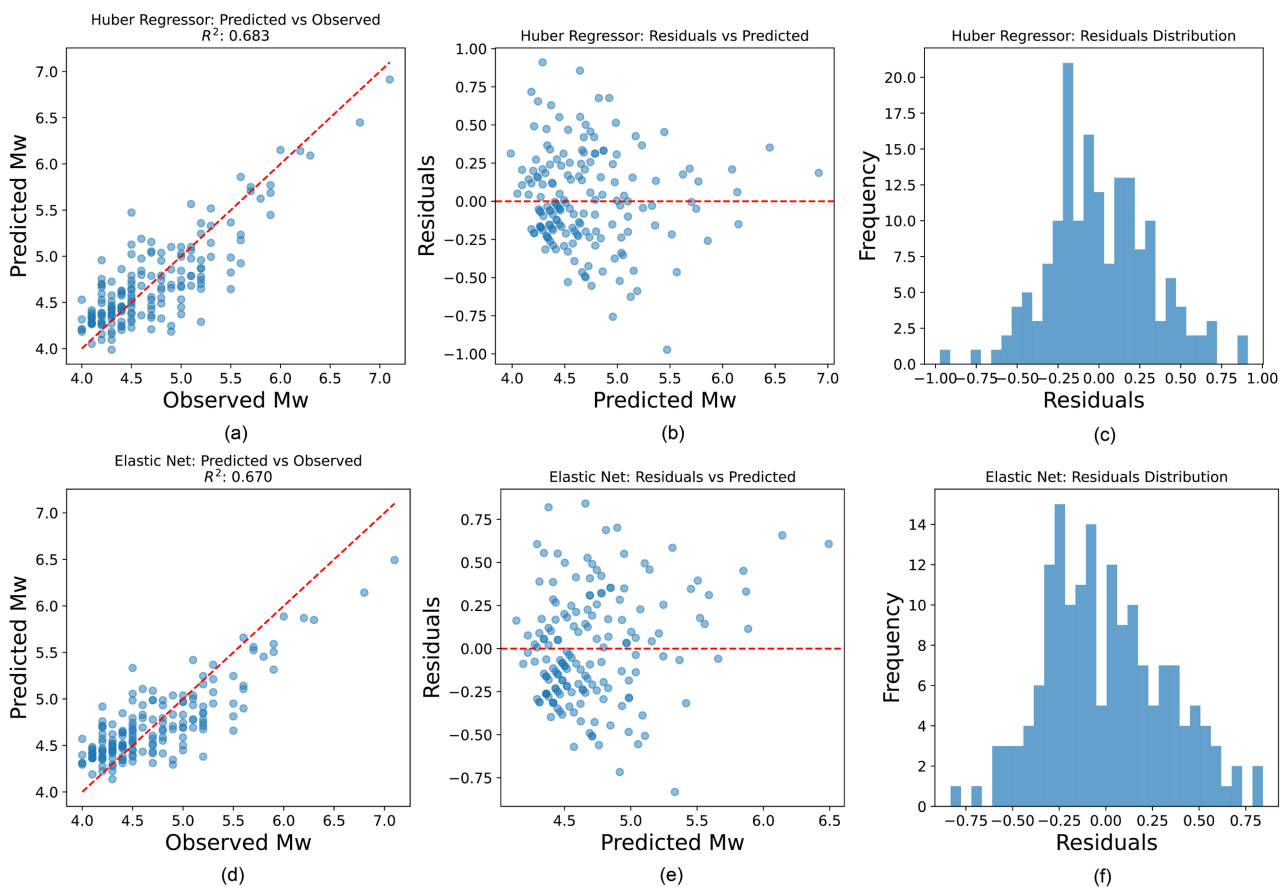
By incorporating bootstrap uncertainty estimation into our tapered Gutenberg-Richter analysis, we constructed a model that acknowledges the fundamental limitations imposed by finite observation periods while providing statistically robust constraints on all parameters that define the region's earthquake magnitude-frequency relationship.

## 4. Seismic Hazard Parameter Estimation

### 4.1. Magnitude Conversion Models

This study employed three different regression methodologies to establish the relationships between moment magnitude ( $M_w$ ) and other parameters (mb, ML). These methods included Multiple Linear Regression (MLR), Huber Regression, and Elastic Net Regression. **Figure 2** presents the performance metrics and diagnostic plots of the three approaches. The analysis revealed that MLR yielded the highest coefficient of determination ( $R^2 = 0.685$ ), followed by Huber Regression ( $R^2 = 0.683$ ) and Elastic Net Regression ( $R^2 = 0.687$ ). The predicted versus observed plots (**Figure 2(a)**, **Figure 2(d)**, **Figure 2(g)**) demonstrated a robust linear correlation between the predicted and actual  $M_w$  values, with data points aggregating around the 1:1 reference line. The minimal variation in the  $R^2$  values suggests comparable performance across the three methods, although MLR exhibited a slightly superior fit to the observed data.

The assessment of residuals offers critical insights into the model performance. Residual plots (**Figure 2(b)**, **Figure 2(e)**, **Figure 2(h)**) demonstrate a relatively even distribution around zero across the predicted values, indicating a minimal systematic bias in the predictions. The residuals from all three techniques approximate Gaussian distributions (**Figure 2(c)**, **Figure 2(f)**, and **Figure 2(i)**), validating the statistical assumptions underlying these methods. A significant finding



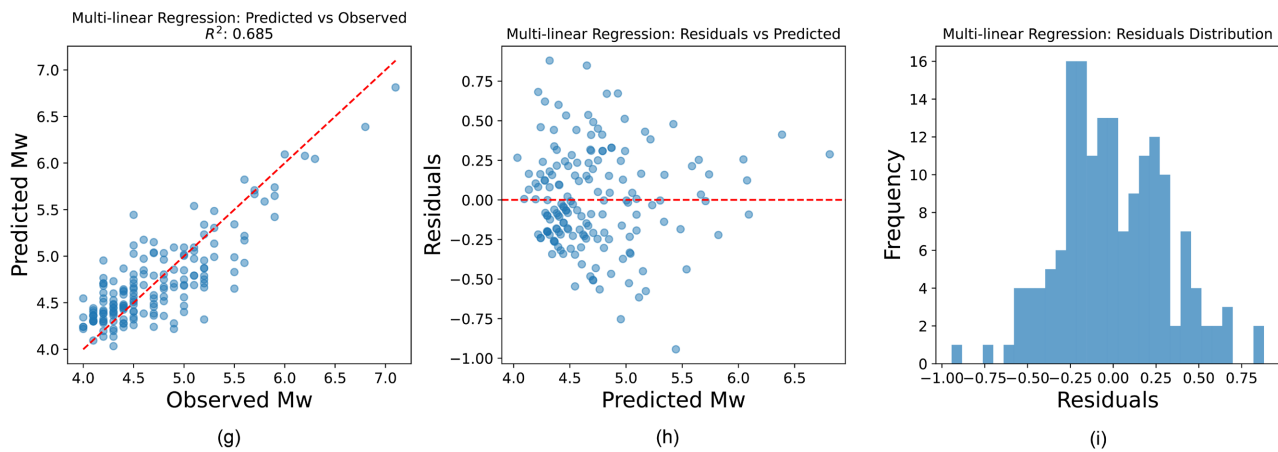


**Figure 2.** Diagnostic plots for the three regression methods used to predict moment magnitude (Mw). Huber Regression results (a)-(c): (a) Predicted versus observed Mw values and 1:1 reference line (red dashed), (b) Residuals versus predicted Mw values showing the distribution of errors, and (c) Histogram of residuals showing their distribution. Elastic Net Regression results (d)-(f): (d) Predicted versus observed Mw values, (e) Residuals versus predicted Mw values, and (f) Distribution of residuals. Multi Linear Regression results (g)-(i): (g) Predicted versus observed Mw values, (h) Residuals versus predicted Mw values, and (i) Distribution of residuals.

from the residual analysis is the slightly higher concentration of data points near zero in the Huber and MLR regression, suggesting improved handling of potential outliers compared to Elastic Net.

Although MLR demonstrated a marginally higher coefficient of determination ( $R^2$ ), the mathematical inclusion of other methods offers several benefits. For instance, Huber Regression offers robust handling of outliers, which renders it particularly suitable for good and reliable earthquake magnitude conversion where data uncertainties are prevalent owing to varying recording conditions and station coverage. Despite its slightly lower  $R^2$ , Elastic Net regression provides valuable regularization that mitigates overfitting, which is especially crucial when dealing with limited dataset sizes typical in regional seismic studies. The consistency across methods and unbiased residuals supports the robustness of these relationships for practical applications in seismic hazard assessments.

#### 4.2. Estimation of $M_c$ , a-value, b-value and $M_{max}$ for the Study Region

Two complementary analytical methods were employed to assess the magnitude completeness and Gutenberg-Richter law parameters for the Nubian-Eurasian plate boundary region: the tapered Gutenberg-Richter model and bootstrap statistics. These parameters are particularly significant in light of recent devastating seismic events within the region.

Application of the tapered Gutenberg-Richter model yielded the following parameter estimates:  $M_c = 4.35$ ,  $a = 6.19$ ,  $b = 0.93$ , corner magnitude = 8.69, and maximum magnitude ( $M_{max}$ ) = 7.24 as shown in **Table 2**. The frequency-magnitude distribution analysis (**Figure 3(a)**) demonstrated a well-defined completeness threshold at  $M_c = 4.35$ , thus validating the completeness of the catalog for

**Table 2.** Results of Tapered Gutenberg-Richter parameters estimated for Nubian-Eurasian Plate Boundary region using two methods.

Method	a-value	b-value	Magnitude of Completeness	$M_{max}$
Maximum Curvature	6.19	0.93	4.35	7.24
Bootstrap Statistics	6.08 (5.35 - 6.90)	0.90 (0.74 - 1.09)	-	7.03 (6.50 - 7.24)

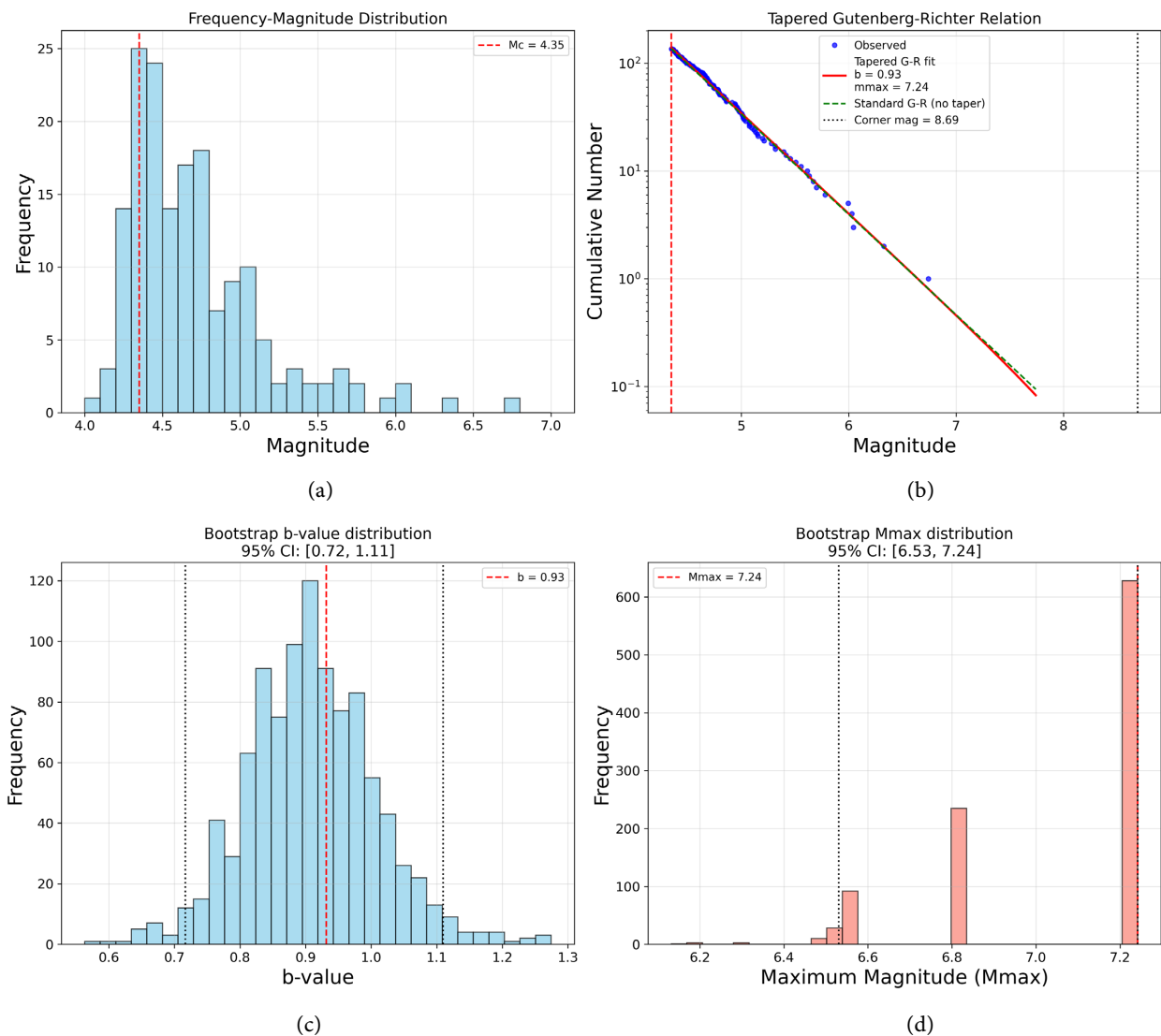


**Figure 3.** Results of the tapered Gutenberg-Richter analysis with bootstrap uncertainty quantification. (a) Frequency-magnitude distribution histogram showing the distribution of earthquakes; the vertical red dashed line indicates  $M_c = 4.35$ . (b) Tapered Gutenberg-Richter relation showing the observed cumulative number of earthquakes (blue dots), tapered G-R fit (red line), standard G-R fit without taper (green dashed line), and corner magnitude (black dotted line); the vertical red dashed line marks the magnitude of completeness. (c) Bootstrap distribution of b-value showing 95% confidence interval; the vertical red dashed line indicates the mean b-value (d) Bootstrap distribution of maximum magnitude ( $M_{max}$ ) showing 95% confidence interval; the vertical red dashed line indicates the estimated  $M_{max}$  of 7.24.

magnitudes exceeding this threshold. The tapered Gutenberg-Richter relationship (**Figure 3(b)**) illustrates how the magnitude-frequency distribution deviates from

the standard linear model at higher magnitudes, providing a more physically realistic representation of the region's seismogenic potential. Notably, **Figure 3(b)** shows excellent agreement between the observed data points and the tapered model fit across the entire magnitude range, resolving the previous discrepancy at higher magnitudes that was evident in the standard G-R model.

The estimated b-value of 0.93 is notable because it falls slightly below the global average of 1.0, suggesting a comparatively higher frequency of large-magnitude seismic events. This observation aligns with the complex tectonic setting of the Nubian-Eurasian plate boundary region, which encompasses multiple active fault systems capable of generating significant earthquakes. The a-value of 6.19 indicates substantial seismic productivity across this extensive plate boundary, reflecting the dynamic tectonic processes actively shaping the region.

The bootstrap analysis provided robust uncertainty quantification for all model parameters, yielding the following 95% confidence intervals: a-value [5.35, 6.90], b-value [0.74, 1.09], corner magnitude [5.77, 8.69], and maximum magnitude [6.50, 7.24]. The bootstrap b-value distribution (**Figure 3(c)**) shows a well-defined, nearly symmetric distribution centered at 0.93, with 95% confidence bounds clearly marked. This distribution demonstrates the statistical robustness of the b-value estimate while acknowledging the inherent uncertainty in parameter estimation. The relatively narrow confidence interval for  $M_{\max}$  suggests good statistical constraint on the upper bound of potential earthquake magnitudes, as visualized in the bootstrap  $M_{\max}$  distribution (**Figure 3(d)**). **Figure 3(d)** reveals a strong peak at 7.24, indicating a high confidence in this maximum magnitude estimate for the region. The corner magnitude of 8.69 indicates where the magnitude distribution begins to deviate significantly from the standard power-law relationship, representing a physical limitation on earthquake size within the region's fault systems.

The bootstrap results demonstrate that while the b-value exhibits moderate uncertainty, the maximum magnitude estimate remains well-constrained. This statistical robustness is particularly valuable for seismic hazard assessment, as it provides a scientifically defensible upper bound for potential earthquake magnitudes. The tapered model's ability to better fit the observed data at higher magnitudes addresses a key limitation of the standard Gutenberg-Richter approach, offering improved characterization of the less frequent but potentially more damaging larger events.

The  $M_{\max}$  value of 7.24 with a lower confidence bound of 6.50 is especially significant given the region's historical seismicity, including the recent Mw 6.8 earthquake in Morocco's High Atlas Mountains. This statistically derived maximum magnitude aligns with geological constraints and historical observations, providing a critical parameter for engineering design criteria and long-term hazard planning across the entire plate boundary region.

These comprehensive seismic parameters enhance our understanding of the region's earthquake potential and provide essential inputs for earthquake prepared-

ness and risk mitigation strategies. By incorporating both the tapered model and bootstrap uncertainty quantification, this analysis offers a more complete and physically realistic characterization of seismic hazard across the diverse tectonic domains comprising the Nubian-Eurasian plate boundary.

## 5. Discussion

The analysis of seismic activity in the Nubian-Eurasian plate boundary province using different magnitude conversion models in combination with Gutenberg-Richter parameters provides substantial insight into the seismic characteristics and hazard threat of the region. The three regression methods used in this work—Multiple Linear Regression, Huber Regression, and Elastic Net Regression—were found to be equally effective, based on the magnitude conversion, as attested to by their respective  $R^2$  values of 0.685, 0.683, and 0.670, with residuals that were consistent with Gaussian distributions. This agreement between these approaches reinforces the reliability of magnitude conversion in this region. In addition, the robust handling of outliers using the Huber regression is a further guarantee of the presence of anomalous recordings, an attribute that proves to be especially important in regions with an inhomogeneous distribution of stations, like the Atlas Mountains.

Application of Gutenberg-Richter analysis using both methods explained major features of seismic activity across the region. Particularly, the calculated b-values are significantly lower than the global value of 1.0, reflecting a higher frequency of seismic events with high magnitudes compared to what one would expect in normal cases. This has major implications for seismic hazard assessment in the region, supporting the country's predisposition towards extremely dangerous earthquake events based on recent seismic activity.

To further our analysis, we utilized bootstrap statistics to obtain robust estimates of all tapered Gutenberg-Richter parameters. This comprehensive statistical approach yielded the following parameters with 95% confidence intervals: a-value of 6.19 [5.35, 6.90], b-value of 0.93 [0.74, 1.09], corner magnitude of 8.69 [5.77, 8.69], and maximum magnitude ( $M_{\max}$ ) of 7.24 [6.50, 7.24]. The importance of these parameters, particularly the  $M_{\max}$  value, should be emphasized given the relatively high seismic potential indicated by the b-value. Together, these parameters define the full frequency-magnitude relationship, from the most common smaller events to the largest possible earthquakes that might occur in the region.

The  $M_c$  value of 4.35 indicates a limitation in the recording of seismic events of lower magnitudes. This suggests the critical need for higher densities of seismic monitoring networks across the region, especially in areas most vulnerable to seismic activity, like the Atlas Mountains and the Rif Zone. Implications of these findings for seismic hazard assessment and mitigation strategies in the region are significant. The comparatively higher  $M_c$  values emphasize the necessity of improved seismic monitoring coverage, especially in the vicinity of population centers and major infrastructure. Moreover, the b-value below 1.0 coupled with a high

a-value of 6.19 indicates substantial seismic productivity with a concerning proportion of larger events, highlighting the urgency for stringent building codes and preparedness strategies.

The corner magnitude of 8.69 represents the point at which the distribution begins to deviate significantly from the standard power-law relationship, providing valuable insight into the physical constraints on earthquake magnitude across this complex plate boundary. This parameter, rarely quantified in traditional seismic analyses, offers important information about the transition point where earthquake frequency begins to taper more rapidly than predicted by the standard Gutenberg-Richter relationship.

Integrating the application of the magnitude conversion model with tapered Gutenberg-Richter analyses and bootstrap uncertainty quantification has led to a comprehensive framework for interpreting the seismic regime of the Nubian-Eurasian plate boundary region. The study suggests that while the present seismic network efficiently monitors moderate and major earthquakes, improvements are necessary for detecting and analyzing small magnitude earthquakes, which could provide vital information on the seismogenic potential of the region.

This research provides a foundation for understanding the seismic hazard features of the region, building a scientifically based framework for increasing earthquake resilience across the plate boundary. By blending different methodologies, the research has produced important outcomes that are relevant for both academic discourse and practical application in risk mitigation across this tectonically active region.

## 6. Conclusion

This study outlines critical relationships between various earthquake magnitude metrics and uses the results to analyze seismic hazard indicators within the Nubian-Eurasian plate boundary region, which has a significant seismic hazard. We overcame the challenge of varied seismic databases and the involvement of incomplete data by geostatistical methods. The results of our work significantly improved the understanding of the seismogenic potential of the region, with particular relevance for seismic events reported in more recent history.

Consistent effectiveness of numerous regression techniques ( $R^2 \approx 0.68$ ) moderately improves the reliability of catalog unification and thus provides a firm foundation for subsequent seismic parameter estimations. Our analysis of Gutenberg-Richter parameters revealed b-values (0.90 - 0.93) that are smaller than the global average, coupled with moderate a-values that vary from 6.08 to 6.19, and an estimate of completeness of magnitude ( $M_c = 4.35$ ) altogether define the seismic setting along the complicated plate boundary. The determined maximum magnitude value of 7.03 (95% CI: 6.50 - 7.24) provides critical constraints for seismic hazard assessment and engineering design within the region.

However, the developed model revealed limitations in providing accurate estimations for low-magnitude seismic events owing to the layout of the existing seis-

mic network. The comparatively higher magnitude of completeness indicates that a considerable portion of the seismic activity for the region remains unobserved, which could affect long-term hazard assessments. Additionally, defining the heterogeneous Nubian-Eurasian boundary as a homogeneous seismotectonic unit with sufficient justification represents a necessary simplification that subsequent research should handle with studies of specific regions. This region encompasses diverse seismotectonic regimes, including extensional zones in the Red Sea, compressional tectonics in the Atlas Mountains, and strike-slip dominated areas in the Dead Sea Transform. Therefore, follow-up research should emphasize the identification of specific sets of seismic parameters for the varying tectonic environments in the boundary region of the Atlas Mountains, the Alboran Sea, and the Rif-Betic. Site conditions and crustal structure must be studied for their effect on magnitude estimations. Additionally, dense local network recordings for higher precision completeness magnitude estimations should be incorporated including investigation of temporal b-value variations as seismic activity predictors, and optimization of techniques for instantaneous magnitude conversion.

This research enables not just the unification of varied seismic events but also provides an extensive framework for understanding seismic hazard factors in the Nubian-Eurasian plate boundary. The findings of the research are of major relevance for the formulation of improved strategies for mitigating risks and provide key seismotectonic knowledge especially relevant for this geologically complex and sociologically important region.

### Conflicts of Interest

The authors declare no conflicts of interest regarding the publication of this paper.

### References

- Agharroud, K., Siame, L. L., Ben Moussa, A., Bellier, O., Guillou, V., Fleury, J., & El Kharim, Y. (2021). Seismo-Tectonic Model for the Southern Pre-Rif Border (Northern Morocco): Insights from Morphochronology. *Tectonics*, *40*, E2020tc006633. <https://doi.org/10.1029/2020TC006633>
- Aki, K. (1965). Maximum Likelihood Estimate of Bin the Formula  $\log N = A - Bm$  and Its Confidence Limits. *Bulletin of the Earthquake Research Institute*, *43*, 237-239.
- Arboleya, M. L., Teixell, A., Charroud, M., & Julivert, M. (2004). A Structural Transect Through the High and Middle Atlas of Morocco. *Journal of African Earth Sciences*, *39*, 319-327. <https://doi.org/10.1016/j.jafrearsci.2004.07.036>
- Bada, G., Cloetingh, S., Gerner, P., & Horváth, F. (1998). Sources of Recent Tectonic Stress in the Pannonian Region: Inferences from Finite Element Modelling. *Geophysical Journal International*, *134*, 87-101. <https://doi.org/10.1046/j.1365-246x.1998.00545.x>
- Beauchamp, W., Allmendinger, R. W., Barazangi, M., Demnati, A., El Alji, M., & Dahmani, M. (1999). Inversion Tectonics and the Evolution of the High Atlas Mountains, Morocco, *Based on A Geological-Geophysical Transect*. *Tectonics*, *18*, 163-184. <https://doi.org/10.1029/1998TC900015>
- Castellaro, S., Mulargia, F., & Kagan, Y. Y. (2006). Regression Problems for Magnitudes. *Geophysical Journal International*, *165*, 913-930.

- <https://doi.org/10.1111/j.1365-246X.2006.02955.x>
- Cherkaoui, T. E., & El Hassani, A. (2012). Seismicity and Seismic Hazard in Morocco. *Bulletin de l'Institut Scientifique, Rabat, Section Sciences de la Terre*, 34, 45-55.
- Chertova, M. V., Spakman, W., Geenen, T., Van Den Berg, A. P., & Van Hinsbergen, D. J. (2014). Underpinning Tectonic Reconstructions of the Western Mediterranean Region with Dynamic Slab Evolution from 3-D Numerical Modeling. *Journal of Geophysical Research: Solid Earth*, 119, 5876-5902. <https://doi.org/10.1002/2014JB011150>
- Efron, B., & Tibshirani, R. J. (1993). *An Introduction to the Bootstrap*. Chapman and Hall/CRC. <https://doi.org/10.1007/978-1-4899-4541-9>
- El Alami, S. O., Tadili, B. A., Cherkaoui, T. E., Medina, F., Ramdani, M., Brahim, L. A., & Harnafi, M. (1998). The Al Hoceima Earthquake of May 26, 1994 and Its Aftershocks: A Seismotectonic Study. *Annals of Geophysics*, 41, 519-537. <https://doi.org/10.4401/ag-3801>
- Eluyemi, A. A., Baruah, S., & Baruah, S. (2019). Empirical Relationships of Earthquake Magnitude Scales and Estimation of Gutenberg–Richter Parameters in Gulf of Guinea Region. *Scientific African*, 6, 1-8. <https://doi.org/10.1016/j.sciaf.2019.e00161>
- Frizon de Lamotte, D., Saint Bezar, B., Bracène, R., & Mercier, E. (2000). The Two Main Steps of the Atlas Building and Geodynamics of the Western Mediterranean. *Tectonics*, 19, 740-761. <https://doi.org/10.1029/2000TC900003>
- Frohlich, C., & Davis, S. D. (1993). Teleseismic *B* Values; or, Much Ado about 1.0. *Journal of Geophysical Research: Solid Earth*, 98, 631-644. <https://doi.org/10.1029/92JB01891>
- Gomez, F., Beauchamp, W., & Barazangi, M. (2000). Role of the Atlas Mountains (North-west Africa) within the African-Eurasian Plate-Boundary Zone. *Geology*, 28, 775-778. [https://doi.org/10.1130/0091-7613\(2000\)28<775:ROTAMN>2.0.CO;2](https://doi.org/10.1130/0091-7613(2000)28<775:ROTAMN>2.0.CO;2)
- Gutenberg, B., & Richter, C. F. (1944). Frequency of Earthquakes in California. *Bulletin of the Seismological Society of America*, 34, 185-188. <https://doi.org/10.1785/BSSA0340040185>
- Hamdache, M., Peláez, J. A., Talbi, A., & López Casado, C. (2010). A Unified Catalog of Main Earthquakes for Northern Algeria from A.D. 856 to 2008. *Seismological Research Letters*, 81, 732-739. <https://doi.org/10.1785/gssrl.81.5.732>
- Helg, U., Burkhard, M., Caritg, S., & Robert-Charrue, C. (2004). Folding and Inversion Tectonics in the Anti-Atlas of Morocco. *Tectonics*, 23, TC4006. <https://doi.org/10.1029/2003TC001576>
- Huber, P. J. (1992). Robust Estimation of a Location Parameter. In S. Kotz, & N. L. Johnson (Eds.), *Breakthroughs in Statistics: Methodology and Distribution* (pp. 492-518). Springer. [https://doi.org/10.1007/978-1-4612-4380-9\\_35](https://doi.org/10.1007/978-1-4612-4380-9_35)
- Kijko, A., & Singh, M. (2011). Statistical Tools for Maximum Possible Earthquake Magnitude Estimation. *Acta Geophysica*, 59, 674-700. <https://doi.org/10.2478/s11600-011-0012-6>
- Koulali, A., Ouazar, D., Tahayt, A., King, R. W., Vernant, P., Reilinger, R. E., McClusky, S., Mourabit, T., Davila, J. M., & Amraoui, N. (2011). New GPS Constraints on Active Deformation Along the Africa-Iberia Plate Boundary. *Earth and Planetary Science Letters*, 308, 211-217. <https://doi.org/10.1016/j.epsl.2011.05.048>
- Lanari, R., Faccenna, C., Fellin, M. G., Essaifi, A., Nahid, A., Medina, F., & Youbi, N. (2020). Tectonic Evolution of the Western High Atlas of Morocco: Oblique Convergence, Reactivation, and Transpression. *Tectonics*, 39, E2019tc005563. <https://doi.org/10.1029/2019TC005563>

- Lasocki, S., & Orlecka-Sikora, B. (2008). Seismic Hazard Assessment Under Complex Source Size Distribution of Mining-Induced Seismicity. *Tectonophysics*, *456*, 28-37. <https://doi.org/10.1016/j.tecto.2006.08.013>
- Mattauer, M., Proust, F., & Tapponnier, P. (1972). Major Strike-Slip Fault of Late Hercynian Age in Morocco. *Nature*, *237*, 160-162. <https://doi.org/10.1038/237160b0>
- Montilla, J. A. P., Hamdache, M., & Casado, C. L. (2003). Seismic Hazard in Northern Algeria Using Spatially Smoothed Seismicity. *Results for Peak Ground Acceleration*. *Tectonophysics*, *372*, 105-119. [https://doi.org/10.1016/S0040-1951\(03\)00234-8](https://doi.org/10.1016/S0040-1951(03)00234-8)
- Mousavi, S. M. (2017). Mapping Seismic Moment and B-Value Within the Continental-Collision Orogenic-Belt Region of the Iranian Plateau. *Journal of Geodynamics*, *103*, 26-41. <https://doi.org/10.1016/j.jog.2016.12.001>
- Orlecka-Sikora, B. (2008). Resampling Methods for Evaluating the Uncertainty of the Non-parametric Magnitude Distribution Estimation in the Probabilistic Seismic Hazard Analysis. *Tectonophysics*, *456*, 38-51. <https://doi.org/10.1016/j.tecto.2007.01.026>
- Pacheco, J. F., Scholz, C. H., & Sykes, L. R. (1992). Changes in Frequency-Size Relationship from Small to Large Earthquakes. *Nature*, *355*, 71-73. <https://doi.org/10.1038/355071a0>
- Peláez, J. A., Chourak, M., Tadili, B. A., Ait Brahim, L., Hamdache, M., López Casado, C., & Martínez Solares, J. M. (2007). A Catalog of Main Moroccan Earthquakes from 1045 to 2005. *Seismological Research Letters*, *78*, 614-621. <https://doi.org/10.1785/gssrl.78.6.614>
- Platt, J. P., Behr, W. M., Johanesen, K., & Williams, J. R. (2013). The Betic-Rif Arc and Its Orogenic Hinterland: A Review. *Annual Review of Earth and Planetary Sciences*, *41*, 313-357. <https://doi.org/10.1146/annurev-earth-050212-123951>
- Poggi, V., Garcia-Peláez, J., Styron, R., Pagani, M., & Gee, R. (2020). A Probabilistic Seismic Hazard Model for North Africa. *Bulletin of Earthquake Engineering*, *18*, 2917-2951. <https://doi.org/10.1007/s10518-020-00820-4>
- Taroni, M., & Carafa, M. M. C. (2023). Earthquake Size Distributions Are Slightly Different in Compression vs Extension. *Communications Earth & Environment*, *4*, Article No. 398. <https://doi.org/10.1038/s43247-023-01059-y>
- Teixell, A., Arbolea, M. L., Julivert, M., & Charroud, M. (2003). Tectonic Shortening and Topography in the Central High Atlas (Morocco). *Tectonics*, *22*, 1-6. <https://doi.org/10.1029/2002TC001460>
- Teixell, A., Barnolas, A., Rosales, I., & Arbolea, M. L. (2017). Structural and Facies Architecture of a Diapir-Related Carbonate Minibasin (Lower and Middle Jurassic, High Atlas, Morocco). *Marine and Petroleum Geology*, *81*, 334-360. <https://doi.org/10.1016/j.marpetgeo.2017.01.003>
- Terrinha, P., Ramos, A., Neres, M., Valadares, V., Duarte, J., Martínez-Loriente, S., Silva, S., Mata, J., Kullberg, J. C., Casas-Sainz, A., & Matias, L. (2019). The Alpine Orogeny in the West and Southwest Iberian Margins. In C. Quesada, & J. T. Oliveira (Eds.), *The Geology of Iberia: A Geodynamic Approach* (pp. 487-505). Springer. [https://doi.org/10.1007/978-3-030-11295-0\\_11](https://doi.org/10.1007/978-3-030-11295-0_11)
- Wiemer, S., & Schorlemmer, D. (2007). ALM: An Asperity-Based Likelihood Model for California. *Seismological Research Letters*, *78*, 134-140. <https://doi.org/10.1785/gssrl.78.1.134>
- Wiemer, S., & Wyss, M. (2000). Minimum Magnitude of Completeness in Earthquake Catalogs: Examples from Alaska, the Western United States, and Japan. *Bulletin of the Seismological Society of America*, *90*, 859-869. <https://doi.org/10.1785/0119990114>
- Zitellini, N., Gràcia, E., Matias, L., Terrinha, P., Abreu, M. A., Dealteris, G., Henriot, J. P.,

Dañobeitia, J. J., Masson, D. G., Mulder, T., & Ramella, R. (2009). The Quest for the Africa-Eurasia Plate Boundary West of the Strait of Gibraltar. *Earth and Planetary Science Letters*, 280, 13-50. <https://doi.org/10.1016/j.epsl.2008.12.005>

Zou, H., & Hastie, T. (2005). Regularization and Variable Selection via the Elastic Net. *Journal of the Royal Statistical Society Series B: Statistical Methodology*, 67, 301-320. <https://doi.org/10.1111/j.1467-9868.2005.00503.x>